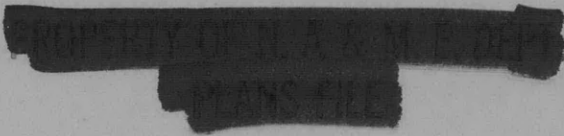


V393
.R46

Report 2308



DEPARTMENT OF THE NAVY



HYDROMECHANICS

THE PRESSURE ON THE SEA BOTTOM DUE TO A
MOVING PRESSURE DISTRIBUTION

AERODYNAMICS

by



V.J. Monacella

and

J.N. Newman

STRUCTURAL
MECHANICS

Distribution of this document is unlimited.

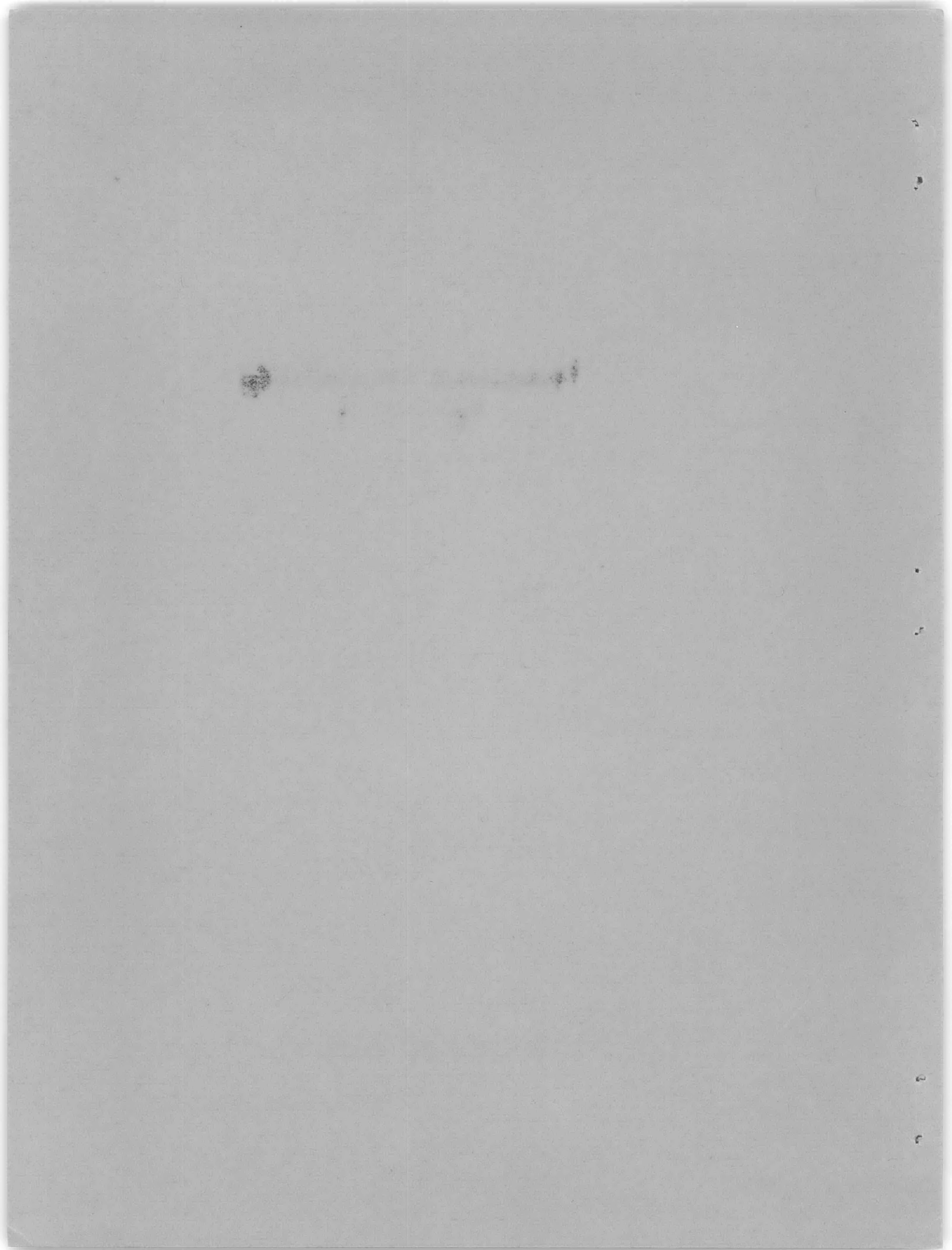
APPLIED
MATHEMATICS

HYDROMECHANICS LABORATORY
RESEARCH AND DEVELOPMENT REPORT

ACOUSTICS AND
VIBRATION

January 1967

Report 2308



DAVID TAYLOR MODEL BASIN
WASHINGTON, D. C. 20007

**THE PRESSURE ON THE SEA BOTTOM DUE TO A
MOVING PRESSURE DISTRIBUTION**

by

V.J. Monacella
and
J.N. Newman

Distribution of this document is unlimited.

January 1967

Report 2308
S-F011 02 32
Task 2382

TABLE OF CONTENTS

	Page
ABSTRACT	1
ADMINISTRATIVE INFORMATION	1
INTRODUCTION	1
MATHEMATICAL FORMULATION OF THE PROBLEM.....	1
SOLUTION OF THE PROBLEM	4
SHALLOW-WATER APPROXIMATION.....	6
NUMERICAL RESULTS	7
APPENDIX A – NUMERICAL EVALUATION OF I_1 AND I_2	14
REFERENCES	16

LIST OF FIGURES

Figure 1 – Coordinate System	3
Figure 2 – Bottom Pressure for $\frac{h}{L} = 1, F = 0.625, \left(\frac{B}{L} = 0.3\right)$	9
Figure 3 – Bottom Pressure for $\frac{h}{L} = 1, F = 0.85, \left(\frac{B}{L} = 0.3\right)$	9
Figure 4 – Bottom Pressure for $\frac{h}{L} = 1, F = 1.5, \left(\frac{B}{L} = 0.3\right)$	10
Figure 5 – Bottom Pressure for $\frac{h}{L} = 1, F = 2, \left(\frac{B}{L} = 0.3\right)$	10
Figure 6 – Bottom Pressure for $\frac{h}{L} = 0.6, F = 0.85, \left(\frac{B}{L} = 0.3\right)$	11
Figure 7 – Bottom Pressure for $\frac{h}{L} = 0.6, F = 1.5, \left(\frac{B}{L} = 0.3\right)$	11
Figure 8 – Comparison of Bottom Pressures at Subcritical and Supercritical Speeds for $\frac{h}{L} = 0.6, \frac{y}{L} = 0, \left(\frac{B}{L} = 0.3\right)$	12

	Page
Figure 9 – Bottom Pressure for $\frac{h}{L} = 0.25, F = 0.625, \left(\frac{B}{L} = 0.3\right)$	12
Figure 10 – Bottom Pressure for $\frac{h}{L} = 0.25, F = 1.5, \left(\frac{B}{L} = 0.3\right)$	13
Figure 11 – Comparison of Exact Theory with Shallow-Water Approximation for $\frac{y}{L} = 0, \left(\frac{h}{L} = 0.1, 0.2, 0.4, 1.1; \frac{B}{L} = 0.3\right)$	13

LIST OF TABLES

Table 1 – Nondimensional Parameters Used in Examples	8
Table 2 – Dimensional Parameters Used in Examples	8

NOTATION

B	Beam of pressure distribution
c	Speed
F	Froude number $\left(\frac{c}{\sqrt{gh}}\right)$
g	Gravitational acceleration
h	Fluid depth
H	Nondimensional depth $\left(2 \frac{h}{L}\right)$
L	Length of pressure distribution
p	Pressure
p_0	Constant base pressure
x, y, z	Rectangular coordinates
β	Beam-length ratio (B/L)
η	Nondimensional coordinate $\left(2 \frac{y}{L}\right)$
ξ	Nondimensional coordinate $\left(2 \frac{x}{L}\right)$
ρ	Fluid mass density

ABSTRACT

The dynamic pressure on the sea bottom due to a constant, rectangular pressure distribution moving at a steady speed over the calm-water surface is determined. The problem is formulated and solved within the framework of potential-flow, linear-wave theory. Numerical results are presented for one beam-to-length ratio, for various water depths, and for both subcritical and supercritical speeds.

ADMINISTRATIVE INFORMATION

This study was supported under Naval Ship Systems Command Subproject S-F011 02 32 Task 2382.

INTRODUCTION

A pressure distribution moving over the calm-water surface will generate both a local disturbance around the distribution itself and a wave system which propagates behind it similar to those caused by a moving ship. Such a surface disturbance will obviously affect the pressure on the sea bottom to an extent depending on the shape and magnitude of the surface disturbance, its velocity, and the depth of water.

The velocity potential associated with a pressure distribution of arbitrary shape moving on the surface of a fluid of finite depth is given by Wehausen and Laitone¹ and, by using Bernoulli's equation, the pressure can be found anywhere in the fluid. If, in particular, the surface distribution is restricted to a rectangular area of constant pressure and if the potential is evaluated on the sea bottom, the analysis is somewhat simplified. Nonetheless, the pressures on the bottom are given in the form of integrals which must be numerically approximated. The necessary numerical analysis and computer programming have been carried out, and the results are presented herein.

Insofar as a moving rectangle of constant pressure is a reasonably good approximation to a ground-effect machine, the bottom pressures presented herein may be interpreted as those due to the passage of such a vehicle. A knowledge of these pressure variations is of interest in the study of pressure-activated mines. Such interest provided the motivation for this investigation.

MATHEMATICAL FORMULATION OF THE PROBLEM

Assume that a constant pressure $p = p_0$ is distributed over a rectangle of length L and width B and that this pressure distribution is moving over the free surface of a fluid of depth

¹References are listed on page 16.

h at a steady speed c parallel to its length. It is required to find the dynamic pressure everywhere on the bottom and for all time. Since the motion is steady with respect to a coordinate system moving with the pressure distribution, the problem can be treated as being independent of time; thus (x, y, z) can be taken to be a right-handed coordinate system moving in space with speed c in the positive x direction. Alternatively, both the pressure distribution and the coordinate system can be taken as fixed in space and with a uniform stream moving with speed c in the negative x direction. In either case the origin of the coordinate system is located in the plane of the undisturbed free surface, the z -coordinate is taken to be positive up, and the pressure distribution occupies the region $|x| \leq \frac{L}{2}$, $|y| \leq \frac{B}{2}$ (Figure 1).

For convenience the constant atmospheric pressure will be taken to be zero so that everywhere on the surface outside the rectangle $p = 0$.*

With the usual assumptions of an inviscid, irrotational fluid there exists a velocity potential Φ , whose positive gradient is equal to the fluid velocity vector; it can be written

$$\Phi(x, y, z) = \phi(x, y, z) - cx$$

where $\phi(x, y, z)$ represents the perturbation potential. It will be further assumed that the disturbance on the surface is sufficiently small so that the problem can be linearized.

The potential $\phi(x, y, z)$ must satisfy the following conditions (see Reference 1):

1. $\nabla^2 \phi = 0$ everywhere in the fluid (Laplace's equation).
2. $\phi_z + \frac{c^2}{g} \phi_{xx} = \frac{c}{\rho g} p_x$ on $z = 0$ (linearized free-surface condition).
3. $\phi_z = 0$ on $z = -h$ (rigid-bottom condition).
4. $\left. \begin{matrix} \phi_x \\ \phi_y \\ \phi_z \end{matrix} \right\} = o(x^{-1/2})$ as $x \rightarrow +\infty$ (radiation condition).

where c is the forward speed of the pressure distribution (alternatively, $c =$ speed of the free stream);

$$p = \begin{cases} p_0 & \text{for } |x| \leq \frac{L}{2} \text{ and } |y| \leq \frac{B}{2} \\ 0 & \text{otherwise} \end{cases};$$

ρ is the fluid density;

g is the gravitational acceleration; and the subscripts designate partial differentiation.

*Note that there is no loss of generality provided the base pressure p_0 is defined relative to atmospheric pressure.

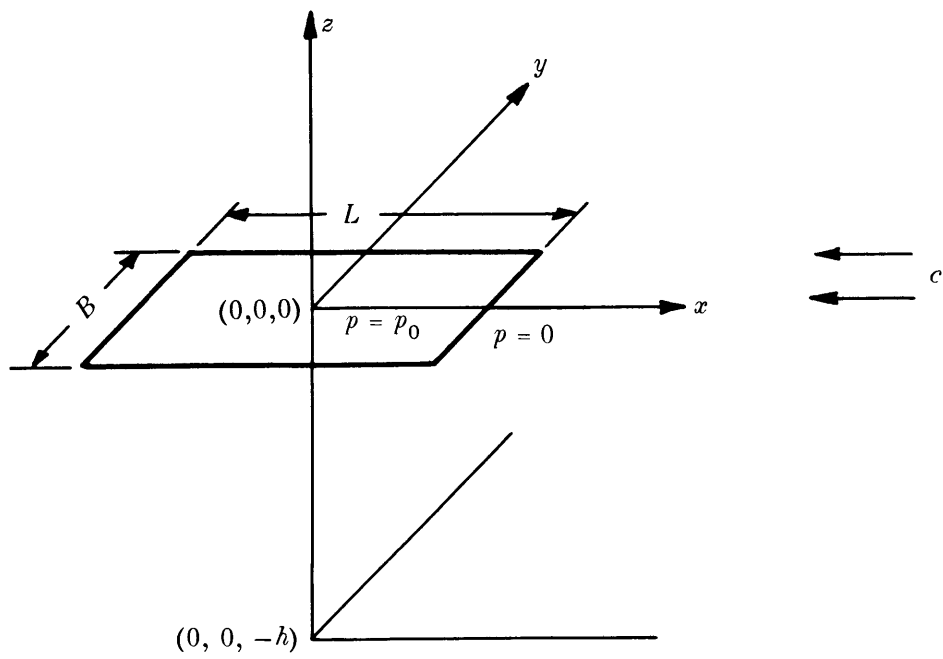


Figure 1 – Coordinate System

SOLUTION OF THE PROBLEM

The potential satisfying the conditions outlined in the previous section is given¹ by

$$\begin{aligned}
 \phi(x, y, z) = & \frac{p_0}{\pi^2 \rho c} \int_{-B/2}^{B/2} \int_{-L/2}^{L/2} d\bar{x} d\bar{y} \int_0^{\pi/2} d\theta \sec \theta \\
 & \int_0^\infty dk \frac{k h \cosh k(z+h) \operatorname{sech} kh}{k h - \frac{1}{F^2} \sec^2 \theta \tanh kh} \sin [k(x - \bar{x}) \cos \theta] \\
 & \cos [k(y - \bar{y}) \sin \theta] \tag{1} \\
 & - \frac{p_0}{\pi \rho c} \int_{-B/2}^{B/2} \int_{-L/2}^{L/2} d\bar{x} d\bar{y} \int_{\theta_0}^{\pi/2} d\theta \sec \theta \\
 & \frac{k_0 \cosh k_0(z+h) \operatorname{sech} k_0 h}{1 - \frac{1}{F^2} \sec^2 \theta \operatorname{sech}^2 k_0 h} \cos [k_0(x - \bar{x}) \cos \theta] \\
 & \cos [k_0(y - \bar{y}) \sin \theta]
 \end{aligned}$$

where $F = \frac{c}{\sqrt{gh}}$ is the Froude number based on depth

$k_0 = k_0(\theta)$ is the positive, real root of $k h - \frac{1}{F^2} \sec^2 \theta \tanh kh = 0$

$$\theta_0 = \begin{cases} \cos^{-1} \left(\frac{1}{F} \right) & \text{for } F > 1 \\ 0 & \text{for } F < 1 \end{cases}$$

and \int means that the integral is to be interpreted as a Cauchy principal value.

If z is set equal to $-h$, and the integration with respect to (\bar{x}, \bar{y}) is carried out, then since

$$\int_{-L/2}^{L/2} d\bar{x} \begin{Bmatrix} \sin [k(x - \bar{x}) \cos \theta] \\ \cos [k(x - \bar{x}) \cos \theta] \end{Bmatrix} = \frac{2}{k \cos \theta} \sin \left(k \frac{L}{2} \cos \theta \right) \begin{Bmatrix} \sin (k x \cos \theta) \\ \cos (k x \cos \theta) \end{Bmatrix}$$

and

$$\int_{-B/2}^{B/2} d\bar{y} \cos [k(y - \bar{y}) \sin \theta] = \frac{2}{k \sin \theta} \sin (k B/2 \sin \theta) \cos (k y \sin \theta)$$

it follows that

$$\begin{aligned} \phi(x, y, -h) &= \frac{4 p_0}{\pi^2 \rho c} \int_0^{\pi/2} d\theta \sec^2 \theta \csc \theta \\ &\int_0^{\infty} dk \frac{k^{-1} h \operatorname{sech} kh}{kh - \frac{1}{F^2} \sec^2 \theta \tanh kh} \sin (k L/2 \cos \theta) \\ &\sin (k B/2 \sin \theta) \sin (k x \cos \theta) \cos (k y \sin \theta) \\ &- \frac{4 p_0}{\pi \rho c} \int_{\theta_0}^{\pi/2} d\theta \sec^2 \theta \csc \theta \frac{k_0^{-1} \operatorname{sech} k_0 h}{1 - \frac{1}{F^2} \sec^2 \theta \operatorname{sech}^2 k_0 h} \\ &\sin (k_0 L/2 \cos \theta) \sin (k_0 B/2 \sin \theta) \cos (k_0 x \cos \theta) \cos (k_0 y \sin \theta) \end{aligned}$$

From Bernoulli's equation, neglecting the steady hydrostatic pressure and second-order terms, the pressure on the bottom is given by $p = \rho c \phi_x$. Thus the ratio of the bottom pressure to that of the constant surface pressure p_0 is given in nondimensional form by

$$\frac{p}{p_0} (\xi, \eta) = \frac{4}{\pi^2} I_1 (\xi, \eta) + \frac{4}{\pi} I_2 (\xi, \eta) \quad [2]$$

where

$$\begin{aligned} I_1 &= \int_0^{\pi/2} d\theta \sec \theta \csc \theta \int_0^{\infty} dK \frac{H \operatorname{sech} KH}{KH - \frac{1}{F^2} \sec^2 \theta \tanh KH} \\ &\sin (K \cos \theta) \sin (K \beta \sin \theta) \cos (K \xi \cos \theta) \cos (K \eta \sin \theta) \\ I_2 &= \int_{\theta_0}^{\pi/2} d\theta \sec \theta \csc \theta \frac{\operatorname{sech} K_0 H}{1 - \frac{1}{F^2} \sec^2 \theta \operatorname{sech}^2 K_0 H} \\ &\sin (K_0 \cos \theta) \sin (K_0 \beta \sin \theta) \sin (K_0 \xi \cos \theta) \cos (K_0 \eta \sin \theta) \end{aligned}$$

Here $\beta = B/L$ is the beam-length ratio

$$\left. \begin{matrix} \xi \\ \eta \\ H \end{matrix} \right\} = 2/L \left\{ \begin{matrix} x \\ y \\ h \end{matrix} \right.$$

and $K_0(\theta)$ satisfies the equation

$$K_0 H - \frac{1}{F^2} \sec^2 \theta \tanh K_0 H = 0$$

It should be noted that I_1 and I_2 are, respectively, even and odd functions of ξ and that they both are even functions of η . Therefore since

$$\frac{p}{p_0}(-\xi, \pm \eta) = \frac{4}{\pi^2} I_1(\xi, \eta) - \frac{4}{\pi} I_2(\xi, \eta)$$

it is sufficient to evaluate the integrals for only positive values of their arguments.

SHALLOW-WATER APPROXIMATION

The limiting value of the pressure ratio p/p_0 as the depth approaches zero is referred to here as the shallow-water approximation. From Equation [2] it can be seen that if $H \rightarrow 0$, $K_0 H \rightarrow 0$, and $F \rightarrow \infty$, then

$$\begin{aligned} \frac{p}{p_0} &\rightarrow \frac{4}{\pi^2} \int_0^{\pi/2} d\theta \sec \theta \csc \theta \int_0^\infty \frac{dK}{K} \sin(K \cos \theta) \sin(K \beta \sin \theta) \\ &\quad \cos(K \xi \cos \theta) \cos(K \eta \sin \theta) \\ &= \frac{1}{4} [\tilde{p}(\xi, \eta) + \tilde{p}(-\xi, \eta) + \tilde{p}(\xi, -\eta) + \tilde{p}(-\xi, -\eta)] \end{aligned}$$

where

$$\begin{aligned} \tilde{p}(\xi, \eta) &= \frac{4}{\pi^2} \int_0^{\pi/2} d\theta \sec \theta \csc \theta \int_0^\infty \frac{dK}{K} \sin [K(1 - \xi) \cos \theta] \sin [K(\beta - \eta) \sin \theta] \\ &= \frac{2}{\pi^2} \int_0^{\pi/2} d\theta \sec \theta \csc \theta \ln \left| \frac{X + \tan \theta}{X - \tan \theta} \right| \operatorname{sgn} [(1 - \xi)(\beta - \eta)] \end{aligned}$$

and

$$X = \left| \frac{1 - \xi}{\beta - \eta} \right|$$

Here $\text{sgn}(x) = \pm 1$ according as $x \gtrless 0$, respectively. With the substitution $q = \frac{1}{X} \tan \theta$ it follows that

$$\tilde{p} = \frac{2}{\pi^2} \int_0^{\infty} \frac{dq}{q} \ln \left| \frac{1+q}{1-q} \right| \text{sgn} [(1-\xi)(\beta-\eta)] = \text{sgn} [(1-\xi)(\beta-\eta)]$$

This leads to the simple result that

$$\frac{p}{p_0} = \begin{cases} 1 & \text{if } |\xi| < 1 \text{ and } |\eta| < \beta \\ 0 & \text{if } |\xi| > 1 \text{ and/or } |\eta| > \beta \end{cases}$$

that is, as one would expect, the pressure p is zero everywhere except directly under the rectangle where it takes the value p_0 .

NUMERICAL RESULTS

As stated before the integrals presented in Equation [2] can only be evaluated numerically. A program for this purpose was written for the IBM 7090 and several examples are given graphically in Figures 2 through 11. Details of the numerical analysis are outlined in the Appendix. All of the calculations are for a beam-length ratio (β) of 0.3. Table 1 shows the values of the remaining parameters pertinent to the various figures.

In order to give some dimensional concept to the figures one can assume the rectangle to be 100 feet long and 30 feet wide. With this configuration, Table 2 shows the dimensions equivalent to the parameters of Table 1.

For subcritical speed* ($F < 1.0$) there is both a transverse and divergent wave system propagated behind the rectangle. As would be expected the oscillations of the centerline ($y/L = 0$) pressure traces of Figures 2, 3, 6, and 9 are similar to those of the transverse wave system. For supercritical speeds there are no transverse waves and, consequently, one would not anticipate an oscillatory behavior of the centerline trace far downstream. Figure 8 shows a comparison of centerline pressures for subcritical and supercritical speeds. Off the centerline, however, the pressure trace can still exhibit an oscillatory pattern due to the diverging wave system. Since the diverging waves are, in general, of shorter length than the transverse waves, the extent to which they affect the bottom pressure depends very

*Critical speed = $\frac{c}{\sqrt{gh}}$.

largely on the depth of water. As can be seen from the figures, typical behavior of a super-critical speed, centerline pressure trace is a building up (from zero) of the pressure near the forepart of the rectangle, a falling off to a negative peak behind it, becoming positive again, and finally approaching zero asymptotically.

The data presented in Figure 11 is intended as a comparison with the shallow-water approximation. In this example $y/L = 0$, while the speed is held constant. The traces are for Froude numbers of 3, 5, 7, and 10. (Recall that in the shallow-water approximation $H \rightarrow 0$ while $F \rightarrow \infty$.) As F increases the abrupt pressure jump at the bow and stern becomes more evident, as predicted in the shallow-water approximation. Also with increasing F the bottom pressure directly under the rectangle appears to be approaching the limiting value of one.

TABLE 1

TABLE 2

Nondimensional Parameters Used in Examples

Dimensional Parameters Used in Examples

Figure	$\frac{h}{L} = \frac{\text{Depth}}{\text{Length}}$	$F = \frac{c}{\sqrt{gh}}$	y/L
2	1.00	0.625	0, 1.0, 2.0
3	1.00	0.85	0, 1.0, 2.0
4	1.00	1.5	0, 1.0, 2.0
5	1.00	2.0	0, 1.0, 2.0
6	0.6	0.85	0, 1.0, 2.0
7	0.6	1.5	0, 0.5, 1.0
8	0.6	0.85, 1.15	0
9	0.25	0.625	0, 0.25, 0.625
10	0.25	1.5	0, 0.25, 0.5
11	0.1, 0.2, 0.4, 1.1	3.0, 5.0, 7.0, 10.0	0

NOTE: $\beta = \frac{\text{Beam}}{\text{Length}} = 0.3$.

Figure	Depth ft	Speed knots	Distance Abeam of Centerline ft
2	100	21.0	0, 100
3	100	28.5	0, 100, 200
4	100	50.4	0, 100, 200
5	100	67.2	0, 100, 200
6	60	22.1	0, 100, 200
7	60	39.0	0, 50, 100
8	60	29.9, 22.1	0
9	25	10.5	0, 25, 62.5
10	25	25.2	0, 25, 50
11	10.0, 20.4, 40.0, 111.1	106.2	0

NOTE: $L = 100$ feet and $B = 30$ feet.

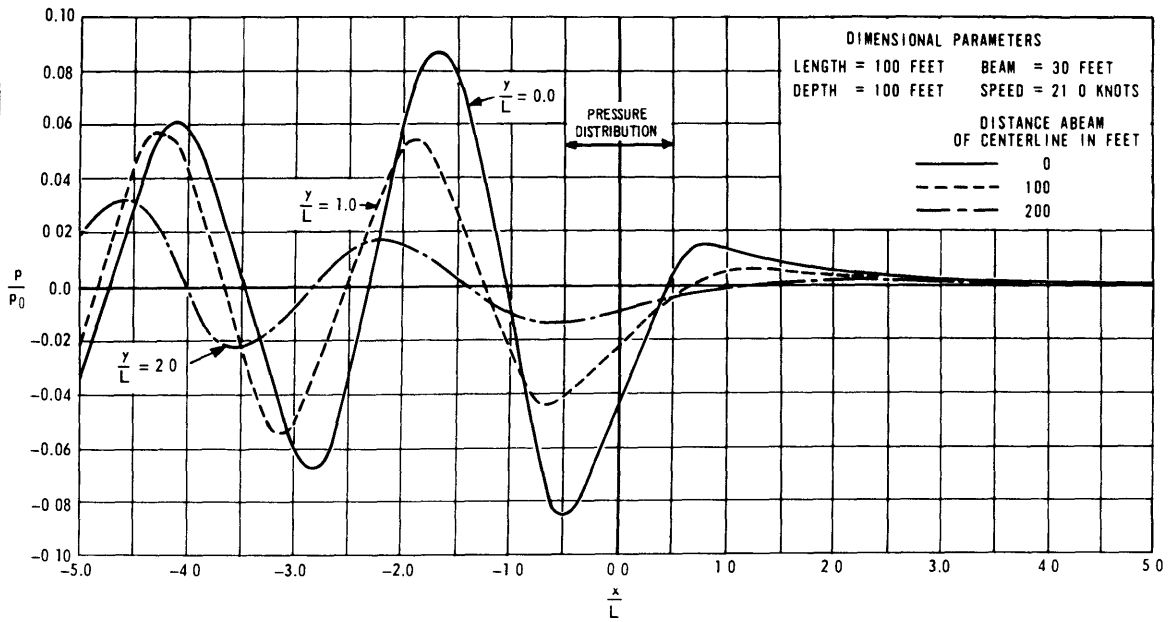


Figure 2 – Bottom Pressure for $\frac{h}{L} = 1.0, F = 0.625 \left(\frac{B}{L} = 0.3 \right)$

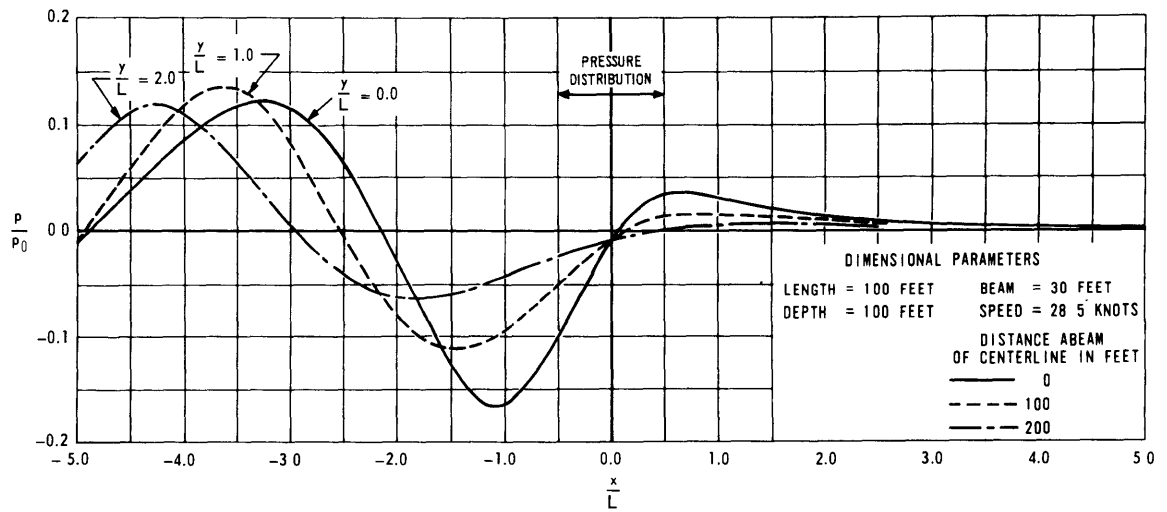


Figure 3 – Bottom Pressure for $\frac{h}{L} = 1.0, F = 0.85 \left(\frac{B}{L} = 0.3 \right)$

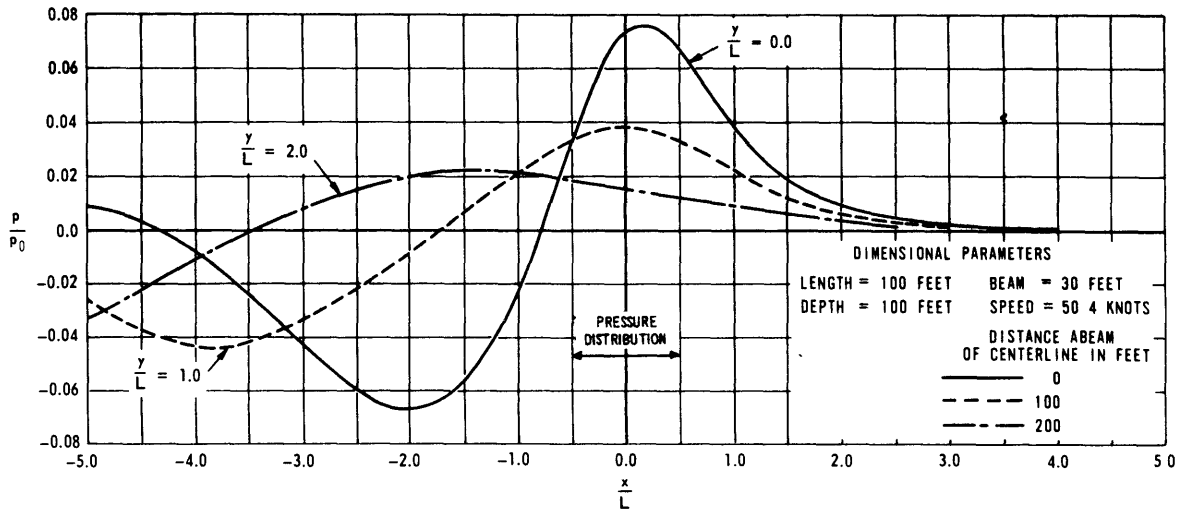


Figure 4 - Bottom Pressure for $\frac{h}{L} = 1.0, F = 1.5 \left(\frac{B}{L} = 0.3 \right)$

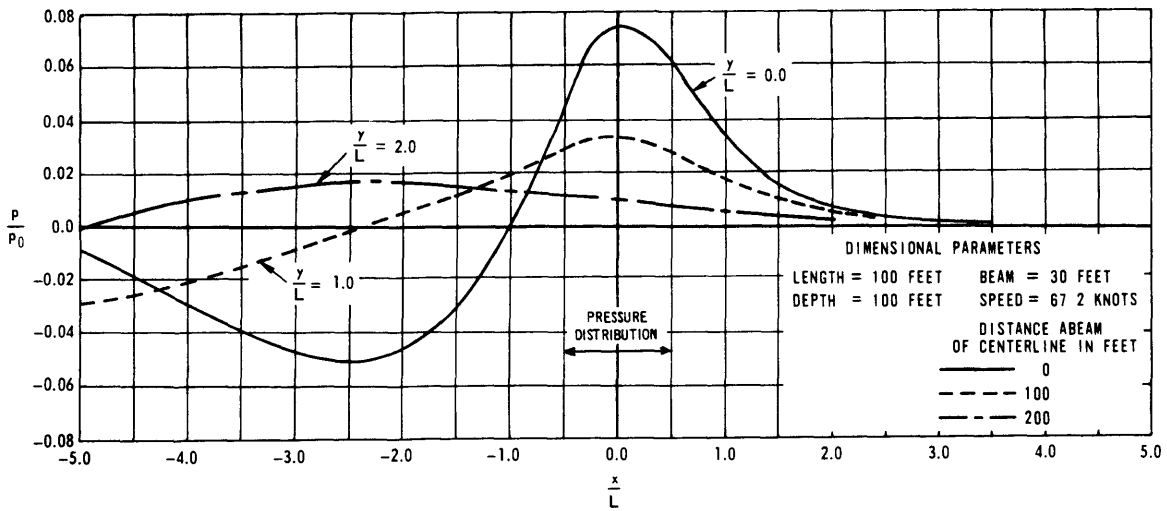


Figure 5 - Bottom Pressure for $\frac{h}{L} = 1.0, F = 2.0 \left(\frac{B}{L} = 0.3 \right)$

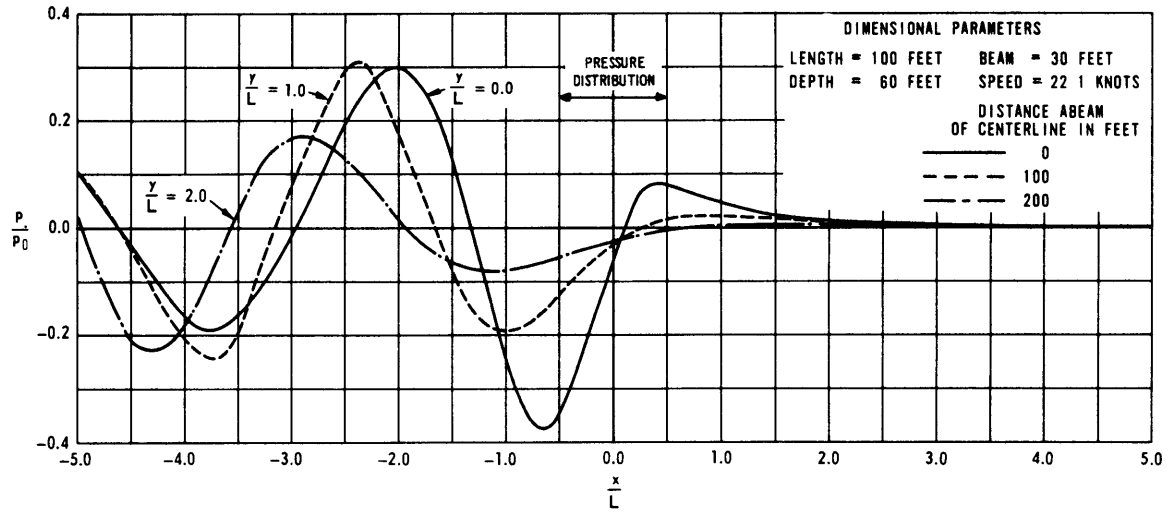


Figure 6 – Bottom Pressure for $\frac{h}{L} = 0.6, F = 0.85 \left(\frac{B}{L} = 0.3 \right)$

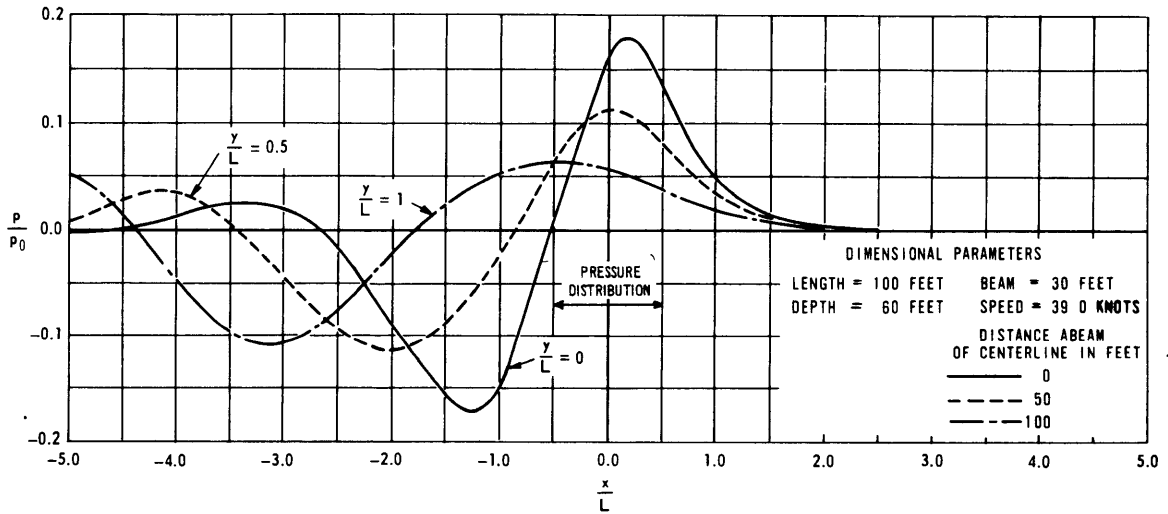


Figure 7 – Bottom Pressure for $\frac{h}{L} = 0.6, F = 1.5 \left(\frac{B}{L} = 0.3 \right)$

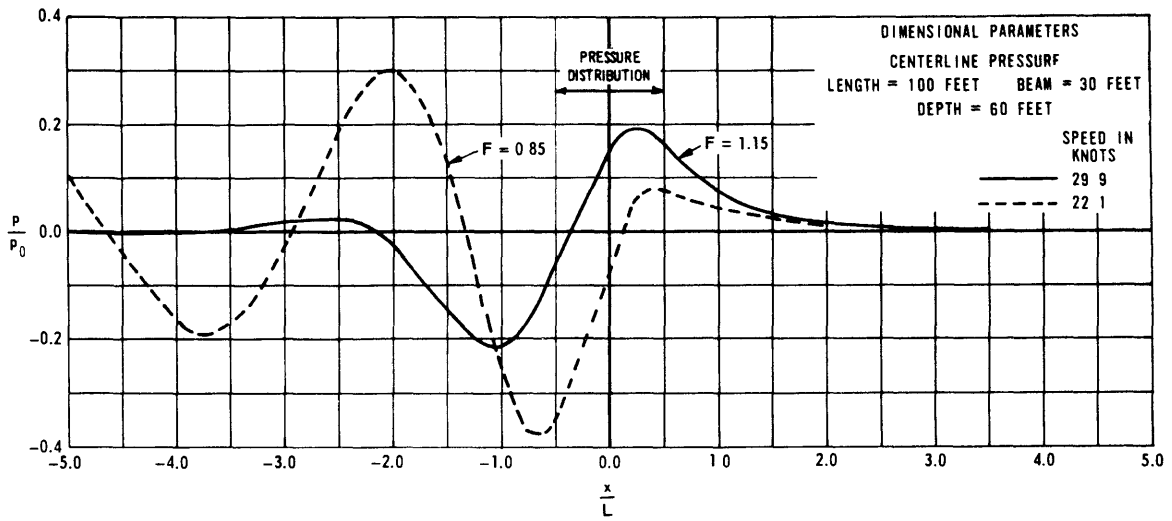


Figure 8 – Comparison of Bottom Pressures at Subcritical and Supercritical Speeds

$$\text{for } \frac{h}{L} = 0.6, \frac{y}{L} = 0 \left(\frac{B}{L} = 0.3 \right)$$

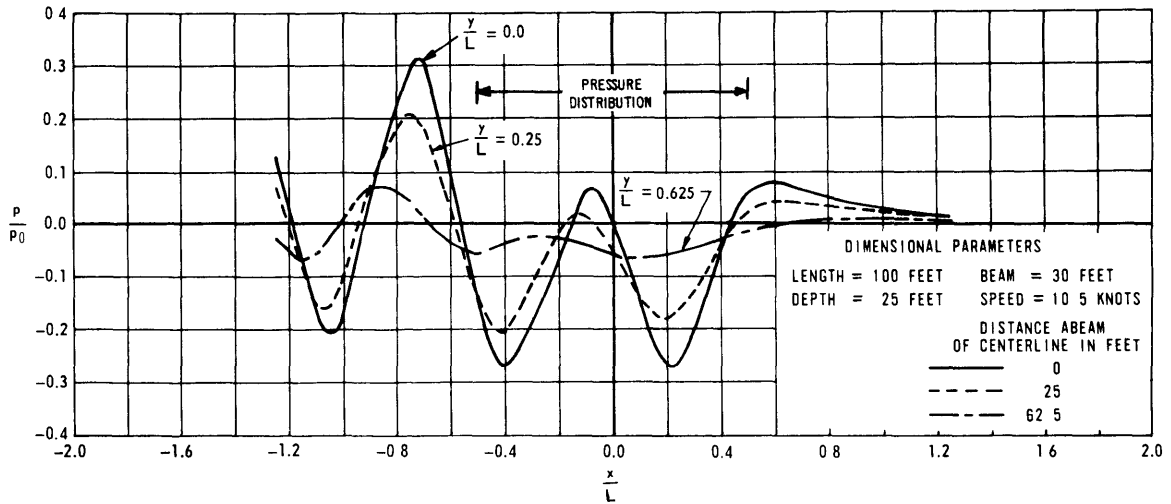


Figure 9 – Bottom Pressure for $\frac{h}{L} = 0.25, F = 0.625 \left(\frac{B}{L} = 0.3 \right)$

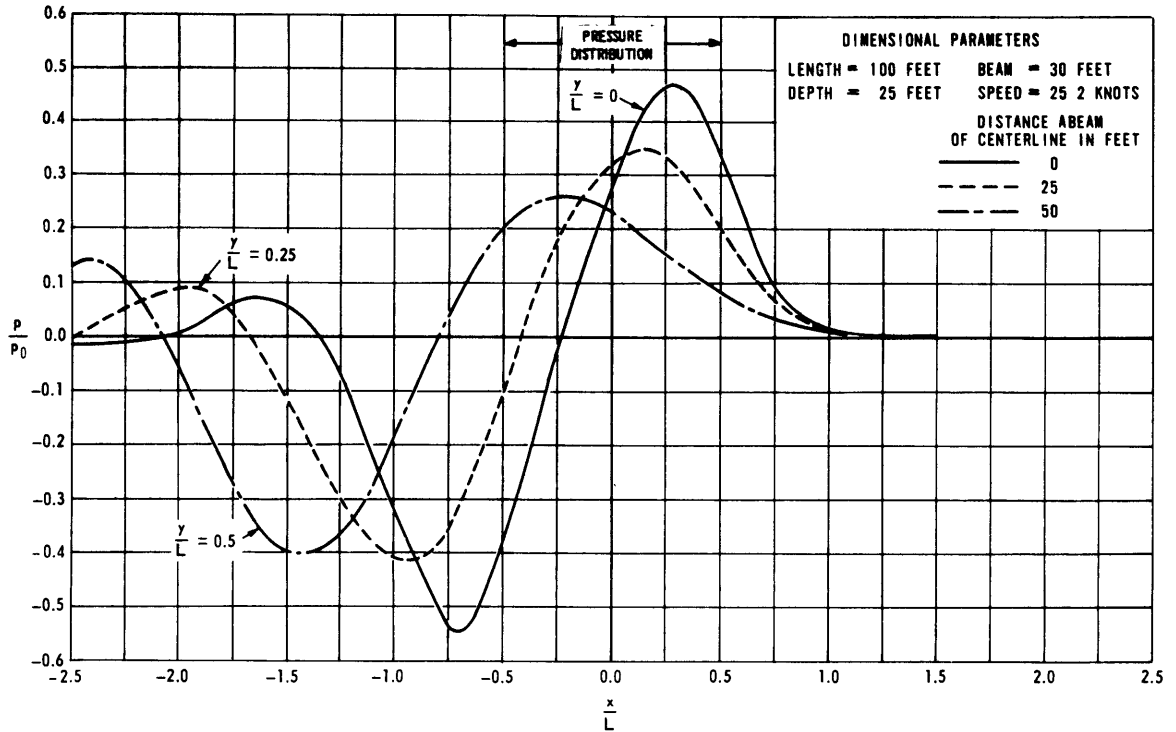


Figure 10 – Bottom Pressure for $\frac{h}{L} = 0.25$, $F = 1.5$ ($\frac{B}{L} = 0.3$)

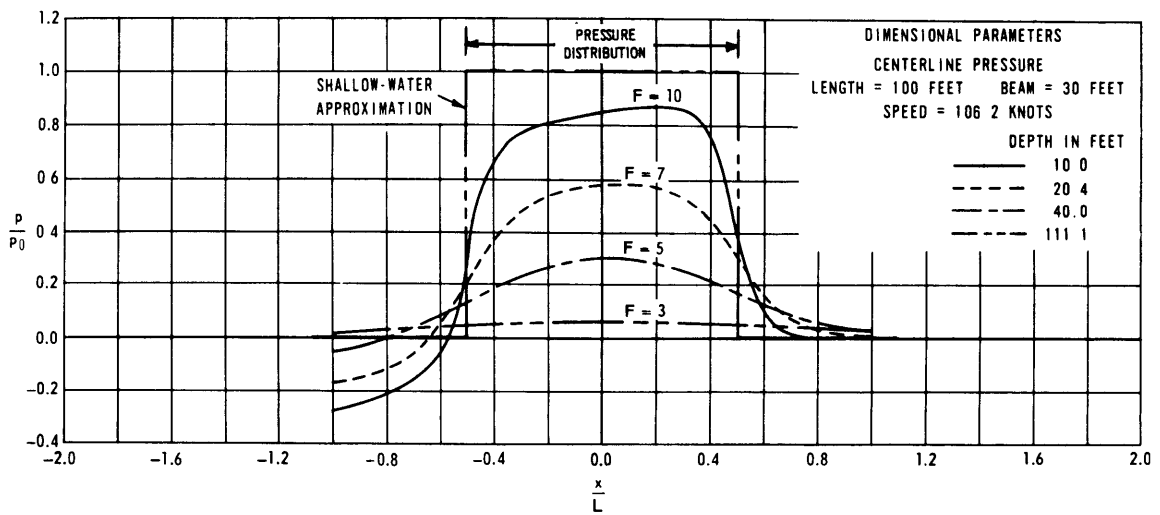


Figure 11 – Comparison of Exact Theory with Shallow-Water Approximation for $\frac{y}{L} = 0$ ($\frac{h}{L} = 0.1, 0.2, 0.4, 1.1$; $\frac{B}{L} = 0.3$)

APPENDIX A

NUMERICAL EVALUATION OF I_1 AND I_2

With the exception of special cases, such as the shallow water approximation, the integrals I_1 and I_2 must be evaluated numerically. A FORTRAN program was written for this purpose, and a summary of the numerical analysis is presented here. For simplicity, and where the meaning is clear, the integrands of the integrals that follow will be omitted.

It was pointed out before that $K_0(\theta)$ is the positive, real root of the transcendental equation $KH - \frac{1}{F^2} \sec^2 \theta \tanh KH = 0$. This root is obtained for each required value of θ by means of the Newton-Raphson method.²

Although the analysis pertaining to the integrals is similar in both cases it is somewhat more convenient to treat subcritical and supercritical speeds separately.

SUBCRITICAL SPEED ($F < 1$)

This is the simpler of the two cases, primarily because $\theta_0 = 0$. For this reason together with the fact that the integrands of both I_1 and I_2 are functions of $\cos \theta$, the θ integrations lend themselves to the Tchebysheff quadrature³ in the form,

$$\int_0^{\pi/2} d\theta f(\cos \theta) \approx \frac{\pi}{2n} \sum_{j=1}^n f(\cos \theta_j)$$

where $\theta_j = \frac{2j-1}{4n} \pi$. In addition to the good accuracy associated with the Gaussian quadrature, it is especially advantageous for computer usage in that both the abscissae and (constant) weight functions can be readily derived within the program. It is used initially for I_2 and the θ integral of I_1 by setting n equal to 10. Then the integrals are reapproximated with n doubled. If the estimates are not sufficiently close as determined by a convergence criterion, n is redoubled, and the process is continued until convergence is obtained.

For each value θ_j of the double integral I_1 the root K_0 is found and the integration on K is performed by first writing the infinite integral as the sum

$$\int_0^{2K_0} dK + \int_{2K_0}^{2K_0+2} dK + \int_{2K_0+2}^{2K_0+4} dK + \dots$$

and approximating each of the integrals in the series by a repeated application of the 10-point Gauss-Legendre quadrature;³ that is, the range of integration of each integral is repeatedly

- subdivided, and the quadrature is applied to each subdivision until convergence is obtained. The series (of integrals) is terminated when the ratio of the absolute value of any one integral to the absolute value of the sum of terms up to that integral is sufficiently small. The first term in the series involves the calculation of a principal value integral but since an even order (10 point) quadrature is used in which the abscissae are symmetric about (but do not include) K_0 , the singularity there can be ignored.⁴

SUPERCRITICAL SPEED ($F > 1$)

The significant differences when $F > 1$ are that $\theta_0 = \cos^{-1} \left(\frac{1}{F} \right)$, and there is a logarithmic singularity at $\theta = \theta_0$ in the integral I_1 . Because of these the Tchebysheff quadrature is not applicable and the 10-point Gauss-Legendre quadrature is used.

The integral I_2 is approximated by the same method described previously, namely, subdividing the range $(\theta_0, \pi/2)$ of integration and applying the quadrature over each subdivision, the number of such subdivisions being whatever is necessary to obtain convergence. The integral I_1 is written as the sum

$$I_1 = I_{11} + I_{12}$$

where

$$I_{11} = \int_0^{\theta_0} d\theta \int_0^{\infty} dK, \text{ and}$$

$$I_{12} = \int_{\theta_0}^{\pi/2} d\theta \int_0^{\infty} dK$$

In both I_{11} and I_{12} the θ integral is approximated by using the Gauss-Legendre quadrature in combination with the 10-point Gaussian quadrature for integrals with a logarithmic singularity.⁵ The integral is approximated in the same way as I_2 , except that the Gauss-Legendre quadrature is used over all the subintervals except the one including θ_0 for which the logarithm quadrature is used.

The K integral of I_{12} is calculated exactly as in the subcritical case. However, for I_{11} it can be readily seen that there is no non-zero root of the transcendental equation and the integrand is well behaved. For this case the integral is written in the same infinite series as before and is approximated exactly the way as for subcritical speed with the exception that $K_0 = 0$.

By the requirement that sufficiently close estimates or of convergence be obtained, a relative error of less than 1 percent is typically implied.

REFERENCES

1. Wehausen, J.V., and Laitone, E.V., "Surface Waves," Handbuch der Physik, Vol. 9, Springer, Berlin, Germany (1960).
2. Hildebrand, F.B., "Introduction to Numerical Analysis," McGraw-Hill Book Company Incorporated, New York (1956), pp. 447-451.
3. Kopal, Z., "Numerical Analysis," Chapman & Hall Ltd, London (1955).
4. Monacella, V.J., "On Ignoring the Singularity in the Numerical Evaluation of Cauchy Principal Value Integrals," David Taylor Model Basin Report 2356 (in preparation).
5. Anderson, D.G., "Gaussain Quadrature Formulae for $\int_0^1 -\ln(x) f(x) dx$," Mathematics of Computation, Vol. 19, No. 91, pp. 477-481 (July 1965).

INITIAL DISTRIBUTION

Copies	Copies
5 NAVSHIPSYSKOM 3 Tech Lib (Code 2921) 1 Appl Res Div (Code 034) 1 Sub (Code 525)	2 COMINLANT
4 NAVSEC 3 Mine Sweeping Br (Code 6631) 1 Prelim Design (Code 6421)	1 COMKWESTEVDDET
1 NAVMAT 1 Lab Mgt (Code 0331)	1 COMOPTEVFOR
2 NAVAIRSYSKOM 1 Aero & Hydro Br (Code AIR 5303) 1 Dyn Sub Unit (Code AIR 530214)	1 NAVSHIPYD NORVA (Acoustic & Pressure Check Range Fort Story, Va.)
3 CO & DIR, USNMDL	1 DIR, Natl BuStand Attn: Dr. Schubauer
6 CHONR 1 Nav Analysis (Code 405) 1 Math Br (Code 432) 2 Fluid Dyn (Code 438) 2 Surf & Amph Prog (Code 463)	20 CDR, DDC
1 ONR, New York	1 DIR, APL, JHUniv
1 ONR, Pasadena	1 DIR, Fluid Mech Lab Univ of California, Berkeley
1 ONR, Chicago	1 DIR, Davidson Lab, SIT
1 ONR, Boston	1 DIR, Inst for Fluid Dyn & Appl Math Univ of Md.
3 CNO 1 (Op-715) 1 (Op-323) 1 (Op-07T)	1 DIR, Hydraul Lab, Univ of Colorado
2 CO & DIR, USNUSL 1 Dr. Pond	1 DIR, Scripps Inst of Oceanography Univ of California
1 CO & DIR, USNEL	1 DIR, ORL, Penn State
2 CDR, USNOL	1 DIR, WHOI
1 DIR, USNRL (Code 5520)	1 Dr. Landweber, Iowa Inst of Hydraul Res
1 CDR, USNOTS, Pasadena	1 DIR, St Anthony Falls Hydraul Lab
2 COMOCEANSYSPAC, Treasure Island	1 Head, NAME, MIT
2 PRES, USNAVWARCOL	1 Inst of Mathematical Sciences New York Univ, New York
2 NAVSCOL MINE WARFARE	2 Dept of Engin, Naval Arch Univ of California, Berkeley 1 Dr. J. Wehausen
2 SUPT, USNAVPGSCOL, Monterey	2 Hydronautics, Inc Pindell School Road Laurel, Md. 1 Dr. Webster
2 COMINPAC	1 Pres, Oceanics, Inc Plainview, New York

Copies

- 1 Dr. Finn Michelsen
Dept of Nav Arch
Univ of Michigan, Ann Arbor
- 1 Dr. T.Y. Wu
Hydro Lab
CIT, Pasadena
- 1 Dr. J. Kotik, TRG, Rt. 110,
Mellville, New York
- 1 Prof. B.V. Korvin-Kroukovsky
East Randolph, Vermont
- 1 Prof. R.L. Wiegel
Univ of California, Berkeley
- 1 Prof. L. Ward, Webb

Security Classification

DOCUMENT CONTROL DATA - R&D

(Security classification of title, body of abstract and indexing annotation must be entered when the overall report is classified)

1. ORIGINATING ACTIVITY (Corporate author) David Taylor Model Basin Washington, D.C. 20007		2a. REPORT SECURITY CLASSIFICATION UNCLASSIFIED	
		2b. GROUP	
3. REPORT TITLE THE PRESSURE ON THE SEA BOTTOM DUE TO A MOVING PRESSURE DISTRIBUTION			
4. DESCRIPTIVE NOTES (Type of report and inclusive dates)			
5. AUTHOR(S) (Last name, first name, initial) Monacella, Vincent J. Newman, J. Nicholas			
6. REPORT DATE January 1967		7a. TOTAL NO. OF PAGES 22	7b. NO. OF REFS 5
8a. CONTRACT OR GRANT NO. b. PROJECT NO. S-F011 02 32 Task 2382 c. d.		9a. ORIGINATOR'S REPORT NUMBER(S) 2308	
		9b. OTHER REPORT NO(S) (Any other numbers that may be assigned this report)	
10. AVAILABILITY/LIMITATION NOTICES Distribution of this document is unlimited.			
11. SUPPLEMENTARY NOTES		12. SPONSORING MILITARY ACTIVITY Naval Ship Systems Command Washington, D.C.	
13. ABSTRACT The dynamic pressure on the sea bottom due to a constant, rectangular pressure distribution moving at a steady speed over the calm-water surface is determined. The problem is formulated and solved within the framework of potential-flow, linear-wave theory. Numerical results are presented for one beam-to-length ratio, for various water depths, and for both subcritical and supercritical speeds.			

Security Classification

14. KEY WORDS	LINK A		LINK B		LINK C	
	ROLE	WT	ROLE	WT	ROLE	WT
Pressure Signatures Ground-Effect Machine Moving Pressure Distribution Pressure-Activated Mines						

INSTRUCTIONS

1. ORIGINATING ACTIVITY: Enter the name and address of the contractor, subcontractor, grantee, Department of Defense activity or other organization (*corporate author*) issuing the report.

2a. REPORT SECURITY CLASSIFICATION: Enter the overall security classification of the report. Indicate whether "Restricted Data" is included. Marking is to be in accordance with appropriate security regulations.

2b. GROUP: Automatic downgrading is specified in DoD Directive 5200.10 and Armed Forces Industrial Manual. Enter the group number. Also, when applicable, show that optional markings have been used for Group 3 and Group 4 as authorized.

3. REPORT TITLE: Enter the complete report title in all capital letters. Titles in all cases should be unclassified. If a meaningful title cannot be selected without classification, show title classification in all capitals in parenthesis immediately following the title.

4. DESCRIPTIVE NOTES: If appropriate, enter the type of report, e.g., interim, progress, summary, annual, or final. Give the inclusive dates when a specific reporting period is covered.

5. AUTHOR(S): Enter the name(s) of author(s) as shown on or in the report. Enter last name, first name, middle initial. If military, show rank and branch of service. The name of the principal author is an absolute minimum requirement.

6. REPORT DATE: Enter the date of the report as day, month, year; or month, year. If more than one date appears on the report, use date of publication.

7a. TOTAL NUMBER OF PAGES: The total page count should follow normal pagination procedures, i.e., enter the number of pages containing information.

7b. NUMBER OF REFERENCES: Enter the total number of references cited in the report.

8a. CONTRACT OR GRANT NUMBER: If appropriate, enter the applicable number of the contract or grant under which the report was written.

8b, 8c, & 8d. PROJECT NUMBER: Enter the appropriate military department identification, such as project number, subproject number, system numbers, task number, etc.

9a. ORIGINATOR'S REPORT NUMBER(S): Enter the official report number by which the document will be identified and controlled by the originating activity. This number must be unique to this report.

9b. OTHER REPORT NUMBER(S): If the report has been assigned any other report numbers (*either by the originator or by the sponsor*), also enter this number(s).

10. AVAILABILITY/LIMITATION NOTICES: Enter any limitations on further dissemination of the report, other than those

imposed by security classification, using standard statements such as:

- (1) "Qualified requesters may obtain copies of this report from DDC."
- (2) "Foreign announcement and dissemination of this report by DDC is not authorized."
- (3) "U. S. Government agencies may obtain copies of this report directly from DDC. Other qualified DDC users shall request through _____."
- (4) "U. S. military agencies may obtain copies of this report directly from DDC. Other qualified users shall request through _____."
- (5) "All distribution of this report is controlled. Qualified DDC users shall request through _____."

If the report has been furnished to the Office of Technical Services, Department of Commerce, for sale to the public, indicate this fact and enter the price, if known.

11. SUPPLEMENTARY NOTES: Use for additional explanatory notes.

12. SPONSORING MILITARY ACTIVITY: Enter the name of the departmental project office or laboratory sponsoring (*paying for*) the research and development. Include address.

13. ABSTRACT: Enter an abstract giving a brief and factual summary of the document indicative of the report, even though it may also appear elsewhere in the body of the technical report. If additional space is required, a continuation sheet shall be attached.

It is highly desirable that the abstract of classified reports be unclassified. Each paragraph of the abstract shall end with an indication of the military security classification of the information in the paragraph, represented as (TS), (S), (C), or (U).

There is no limitation on the length of the abstract. However, the suggested length is from 150 to 225 words.

14. KEY WORDS: Key words are technically meaningful terms or short phrases that characterize a report and may be used as index entries for cataloging the report. Key words must be selected so that no security classification is required. Identifiers, such as equipment model designation, trade name, military project code name, geographic location, may be used as key words but will be followed by an indication of technical context. The assignment of links, roles, and weights is optional.

UNCLASSIFIED

Security Classification

David Taylor Model Basin. Report 2308.

THE PRESSURE ON THE SEA BOTTOM DUE TO A MOVING PRESSURE DISTRIBUTION, by V.J. Monacella and J.N. Newman. Jan 1967. iv, 18p. illus., graphs, diags., refs. UNCLASSIFIED

The dynamic pressure on the sea bottom due to a constant, rectangular pressure distribution moving at a steady speed over the calm-water surface is determined. The problem is formulated and solved within the framework of potential-flow, linear-wave theory. Numerical results are presented for one beam-to-length ratio, for various water depths, and for both subcritical and supercritical speeds.

1. Ground-effect vehicles--
Pressure signatures
- I. Monacella, Vincent J.
- II. Newman, J. Nicholas
- III. S-F011 02 32; Task 2382

David Taylor Model Basin. Report 2308.

THE PRESSURE ON THE SEA BOTTOM DUE TO A MOVING PRESSURE DISTRIBUTION, by V.J. Monacella and J.N. Newman. Jan 1967. iv, 18p. illus., graphs, diags., refs. UNCLASSIFIED

The dynamic pressure on the sea bottom due to a constant, rectangular pressure distribution moving at a steady speed over the calm-water surface is determined. The problem is formulated and solved within the framework of potential-flow, linear-wave theory. Numerical results are presented for one beam-to-length ratio, for various water depths, and for both subcritical and supercritical speeds.

1. Ground-effect vehicles--
Pressure signatures
- I. Monacella, Vincent J.
- II. Newman, J. Nicholas
- III. S-F011 02 32; Task 2382

David Taylor Model Basin. Report 2308.

THE PRESSURE ON THE SEA BOTTOM DUE TO A MOVING PRESSURE DISTRIBUTION, by V.J. Monacella and J.N. Newman. Jan 1967. iv, 18p. illus., graphs, diags., refs. UNCLASSIFIED

The dynamic pressure on the sea bottom due to a constant, rectangular pressure distribution moving at a steady speed over the calm-water surface is determined. The problem is formulated and solved within the framework of potential-flow, linear-wave theory. Numerical results are presented for one beam-to-length ratio, for various water depths, and for both subcritical and supercritical speeds.

1. Ground-effect vehicles--
Pressure signatures
- I. Monacella, Vincent J.
- II. Newman, J. Nicholas
- III. S-F011 02 32; Task 2382

David Taylor Model Basin. Report 2308.

THE PRESSURE ON THE SEA BOTTOM DUE TO A MOVING PRESSURE DISTRIBUTION, by V.J. Monacella and J.N. Newman. Jan 1967. iv, 18p. illus., graphs, diags., refs. UNCLASSIFIED

The dynamic pressure on the sea bottom due to a constant, rectangular pressure distribution moving at a steady speed over the calm-water surface is determined. The problem is formulated and solved within the framework of potential-flow, linear-wave theory. Numerical results are presented for one beam-to-length ratio, for various water depths, and for both subcritical and supercritical speeds.

1. Ground-effect vehicles--
Pressure signatures
- I. Monacella, Vincent J.
- II. Newman, J. Nicholas
- III. S-F011 02 32; Task 2382

MIT LIBRARIES

DUPL



3 9080 02753 0804

10-1-2

10-1-2

10-1-2